



Evaluation of WRF for Forecasting Wind Turbine Icing

Davis, Neil; Hahmann, Andrea N.; Clausen, Niels-Erik; Zagar, Mark

Publication date:
2012

[Link back to DTU Orbit](#)

Citation (APA):

Davis, N., Hahmann, A. N., Clausen, N-E., & Zagar, M. (2012). *Evaluation of WRF for Forecasting Wind Turbine Icing*. Poster session presented at 13th Annual WRF Users' Workshop, Boulder, CO, United States.

General rights

Copyright and moral rights for the publications made accessible in the public portal are retained by the authors and/or other copyright owners and it is a condition of accessing publications that users recognise and abide by the legal requirements associated with these rights.

- Users may download and print one copy of any publication from the public portal for the purpose of private study or research.
- You may not further distribute the material or use it for any profit-making activity or commercial gain
- You may freely distribute the URL identifying the publication in the public portal

If you believe that this document breaches copyright please contact us providing details, and we will remove access to the work immediately and investigate your claim.

Introduction



Figure 1. Photo illustrating Ice shedding & accretion on a turbine in Grenchenburg Sweden (Lasko et al, 2010).

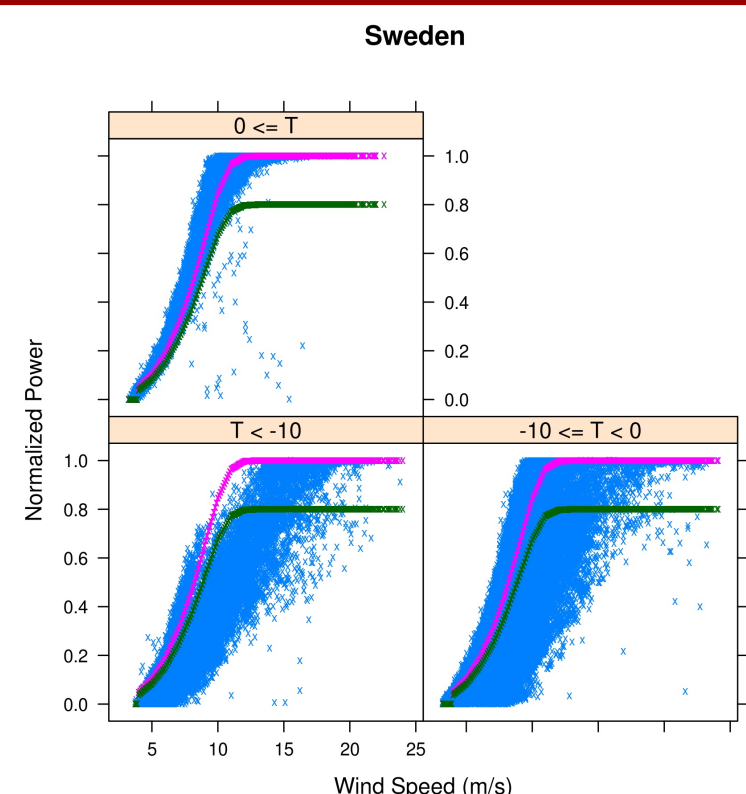


Figure 2. Wind turbine power curve at different air temperatures. The deviation from the power curve at colder temperatures is believed to be the result of icing.

The growth of ice on a wind turbine can pose it many problems. Icing can create a potential safety risk due to ice shedding (fig. 1), lead to production losses which reduce profits (fig. 2), and can increase loads, thereby reducing the turbine lifetime. The ability to forecast turbine icing (fig. 3) could help to minimize these risks both by identifying sites prone to icing during the planning phase, and estimating production losses in the short term.

For this study we examine icing events at a site in Northern Sweden (fig. 4), using WRF and a variety of icing models, in a hind-cast setup for the month of January 2011. The WRF simulated temperature was evaluated against GDAS data over the entire 10 km domain. For evaluating the icing model we utilized production data from 43 of the 47 turbines in the wind park. We utilized the production to estimate observed icing by identifying times where the observed power deviated from the generic power curve by more than 20% and the temperature was below freezing temperature. We then created three observational data-sets depending on how many of the turbines showed the icing signal (all, majority, or any).

We found that WRF does a reasonable job capturing the occurrence of icing found at this site, using the Thompson MP Scheme. We also found that both icing occurrence and amount is highly sensitive to the PBL and microphysics schemes used.

Icing Forecast System

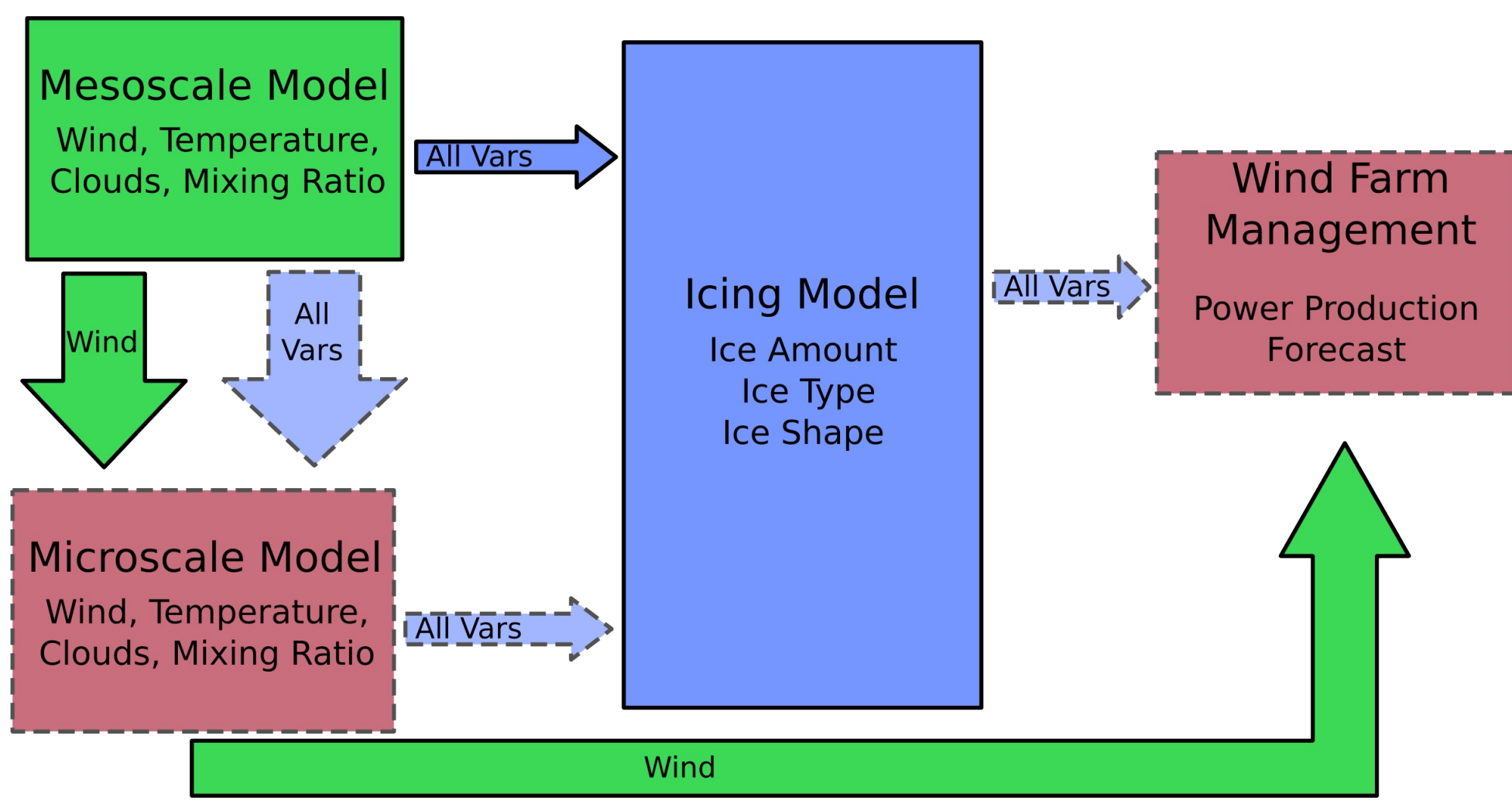


Figure 3. Illustration of a wind turbine power forecasting system which includes icing.

Green objects: Pre-existing
Red objects: Need update for icing
Blue objects: New for icing model

Dashed lines signify items still in need of development / updating.

This study focuses on the mesoscale model & icing model.

Meteorological Model Setup

The WRF model was used to provide meteorological input to the icing models. The model was run over 2 domains at 30 km and 10 km resolution respectively (fig. 3). The outer domain was nudged using the NCEP FNL data-set, which was also used for the input and boundary conditions. Nine sensitivities testing three combinations each of the microphysics and PBL schemes in the model (Table 1).

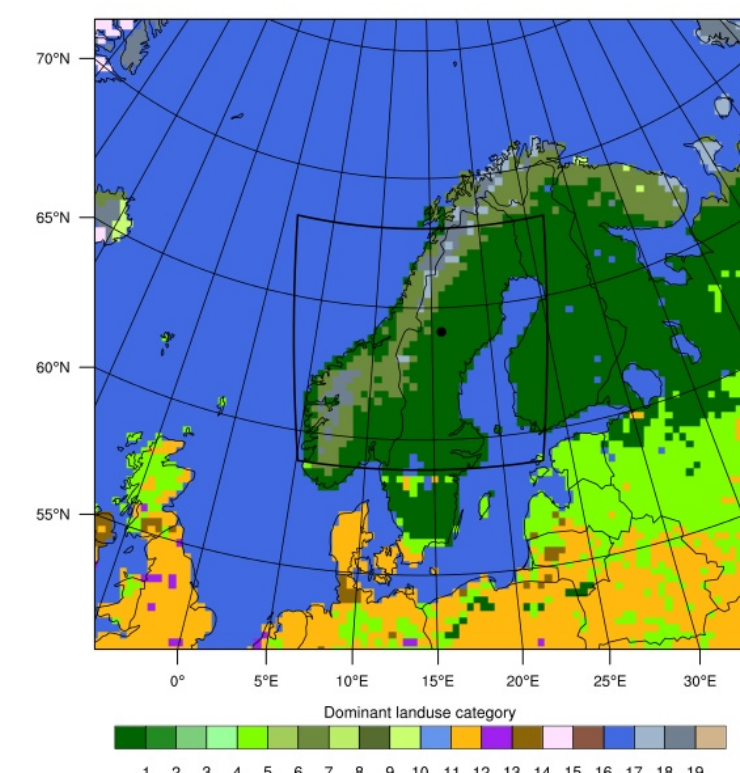


Figure 4: Landuse categories, WRF outer and inner (Black line) domains and location of wind farm used for the study (dot).

Table 1. PBL & microphysical schemes used in the study

Microphysics	SUNY-Lin (13)	Thompson (8)	WSM5 (4)
PBL	MYJ (2)	MYNN2 (5)	YSU (1)

Icing Model

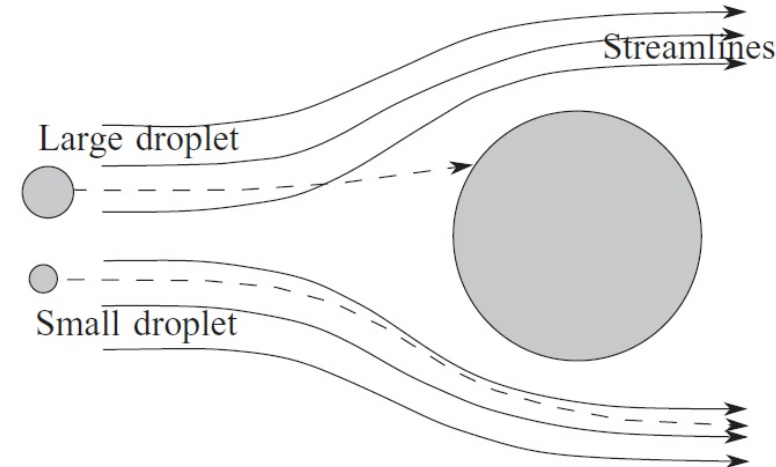


Figure 4. Illustration of how droplet size impacts the trajectory of a particle in flow around an obstacle (Makkonen, 2000).

Collision Efficiency: Percentage of mass flux which impacts the object. A function of wind speed, droplet size (MVD) and object size. Current model is based on flow around a cylinder (Term α_1 from Makkonen, 2000).

Ice Ablation: Melting/evaporation, sublimation or shedding of ice

Kjeller Model: Evaporation / sublimation based on cloud droplets, additional energy from short and long wave radiation budgets, multiplier used to approximate shedding.

DTU Model: Similar to Kjeller with more advanced heat transfer coefficient calculation for airfoils, inclusion of temperature impact on energy budget, no shedding.

TShed: Shedding only model, removes all ice when temperature is 0.5 degrees above freezing

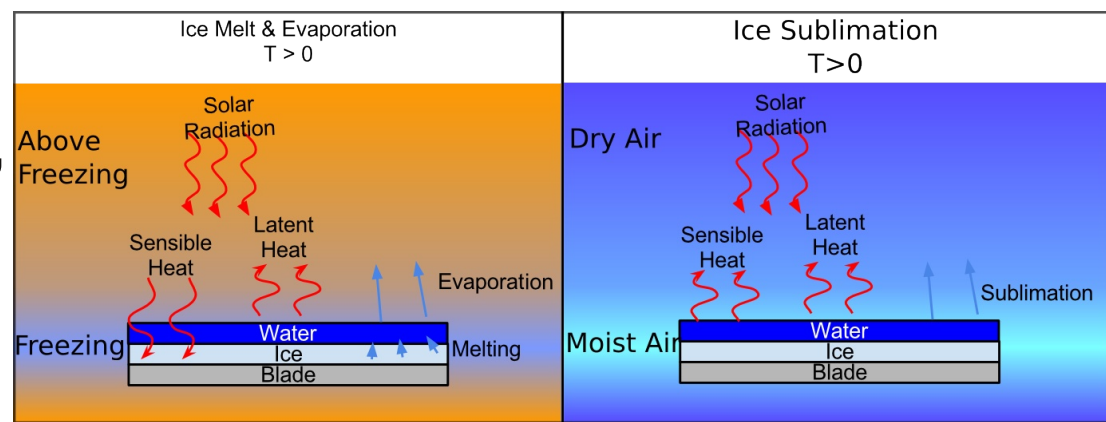


Figure 6. Illustration of the energy (red) and mass (blue) flows for ice undergoing ablation via melting or sublimation.

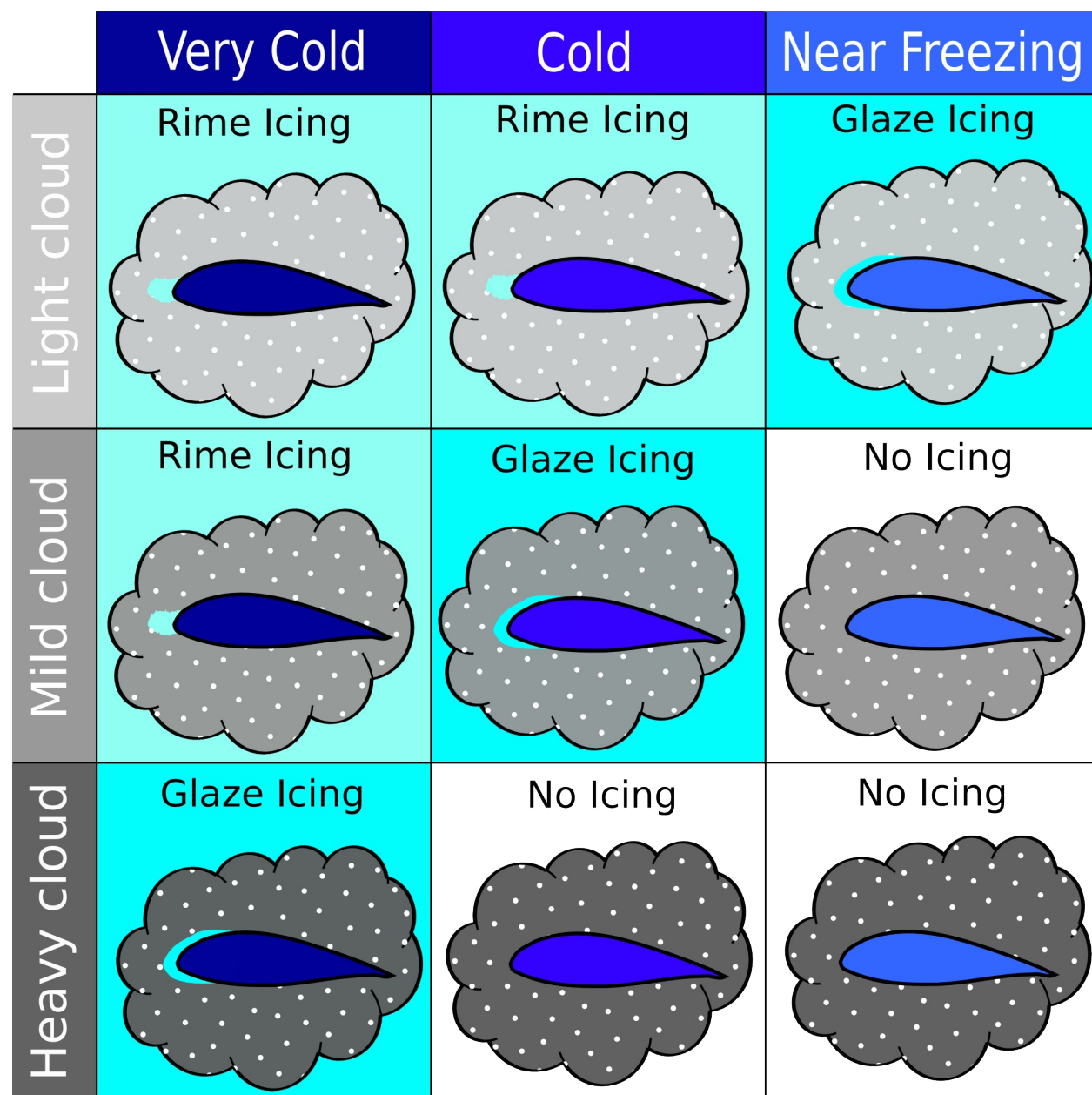


Figure 5. Illustration of the impact of changes to temperature or mass flux on the type of icing experienced by a turbine blade.

Ice Accretion: Growth of ice, function of the heat balance between the heat released via the phase change and other parameters.

Fig. 5 shows the balance required between the mass flux and temperature to maintain each type of icing.

Makkonen: ISO standard model for calculating ice accretion on structures (Makkonen, 2000).

Brakel: Asymptotic model, advanced features: Type of icing, amount of water during glaze icing, ability to represent heating from below (Brakel et al 2000).

WRF Model Evaluation

Table 2. Evaluation of events where the temperature was below 0.

	MYJ	MYNN2	YSU
WSM5	Hit Rate: 0.97 False Alarm: 0.29 Mean Error: -1.35	Hit Rate: 0.94 False Alarm: 0.20 Mean Error: -0.67	Hit Rate: 0.92 False Alarm: 0.14 Mean Error: -0.07
Thom	Hit Rate: 0.97 False Alarm: 0.28 Mean Error: -0.89	Hit Rate: 0.93 False Alarm: 0.18 Mean Error: 0.25	Hit Rate: 0.90 False Alarm: 0.12 Mean Error: 0.56
SUNY-Lin	Hit Rate: 0.96 False Alarm: 0.27 Mean Error: -1.22	Hit Rate: 0.92 False Alarm: 0.19 Mean Error: -0.67	Hit Rate: 0.89 False Alarm: 0.12 Mean Error: 0.31

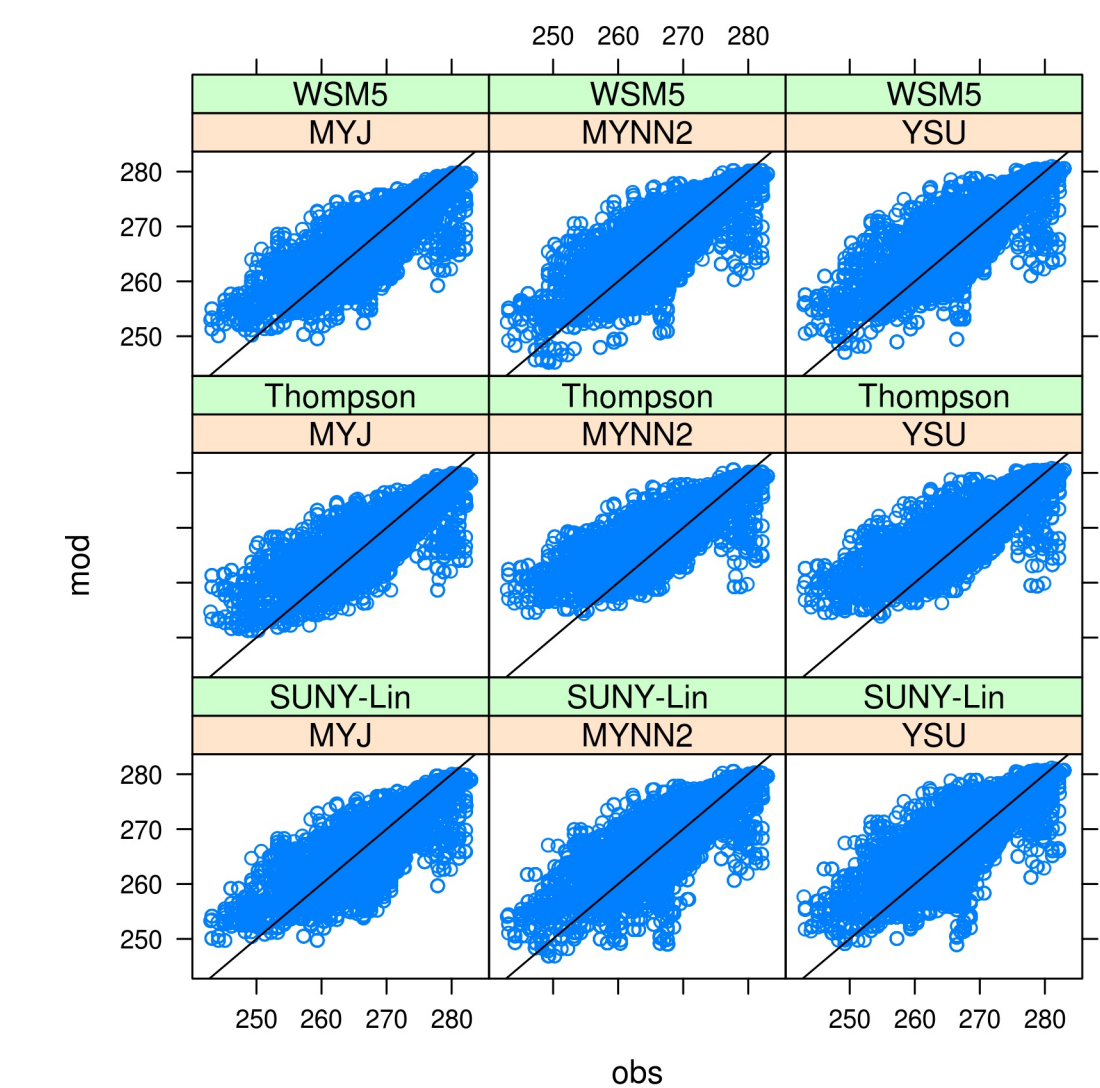


Figure 7. Observed vs WRF simulated temperature at 80m for the nine sensitivity simulations.

The 80m Temperature simulated by the WRF model was evaluated against GDAS data using the MET model evaluation tool. Results shown in Fig. 7 and table 2, show that both the PBL and microphysical scheme influence the model results.

The Thompson and YSU schemes showed the warmest temperatures, while WSM5 & MYNN2 were consistently the coldest. All model runs did a reasonable job estimating freezing temperatures, but the MYJ scheme showed a very high false alarm rate.

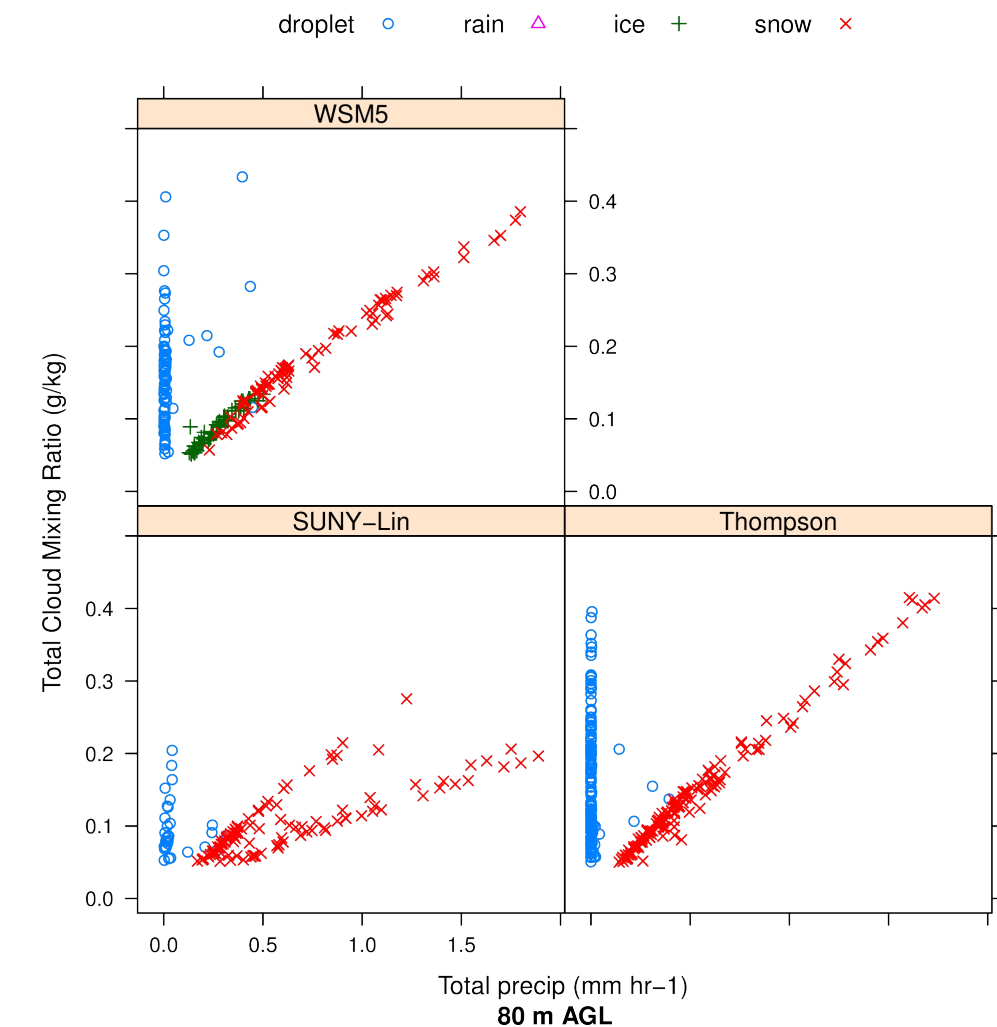


Figure 8. Comparison of the cloud amount at 80m with the total precipitation at the ground. Colors indicate dominant hydrometer type.

Due to the linear increase in cloud amount with precipitation we do not feel the icing model needs precipitation included as a separate input.

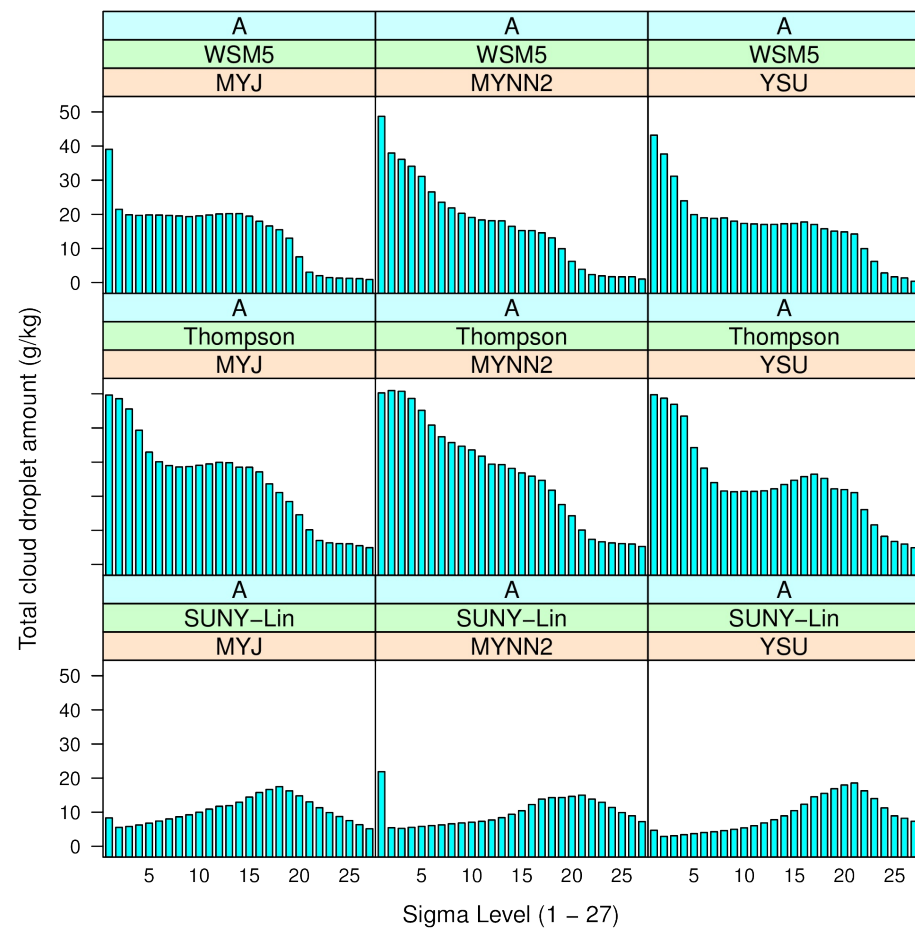


Figure 9. The change in total cloud mixing ratio with height, at a nearby wind farm in Sweden.

We examined this parameter at several locations, and found that the shape of the plots varied mostly due to the site location. However the SUNY-Lin scheme always produced the lowest values.

Ice Model Evaluation

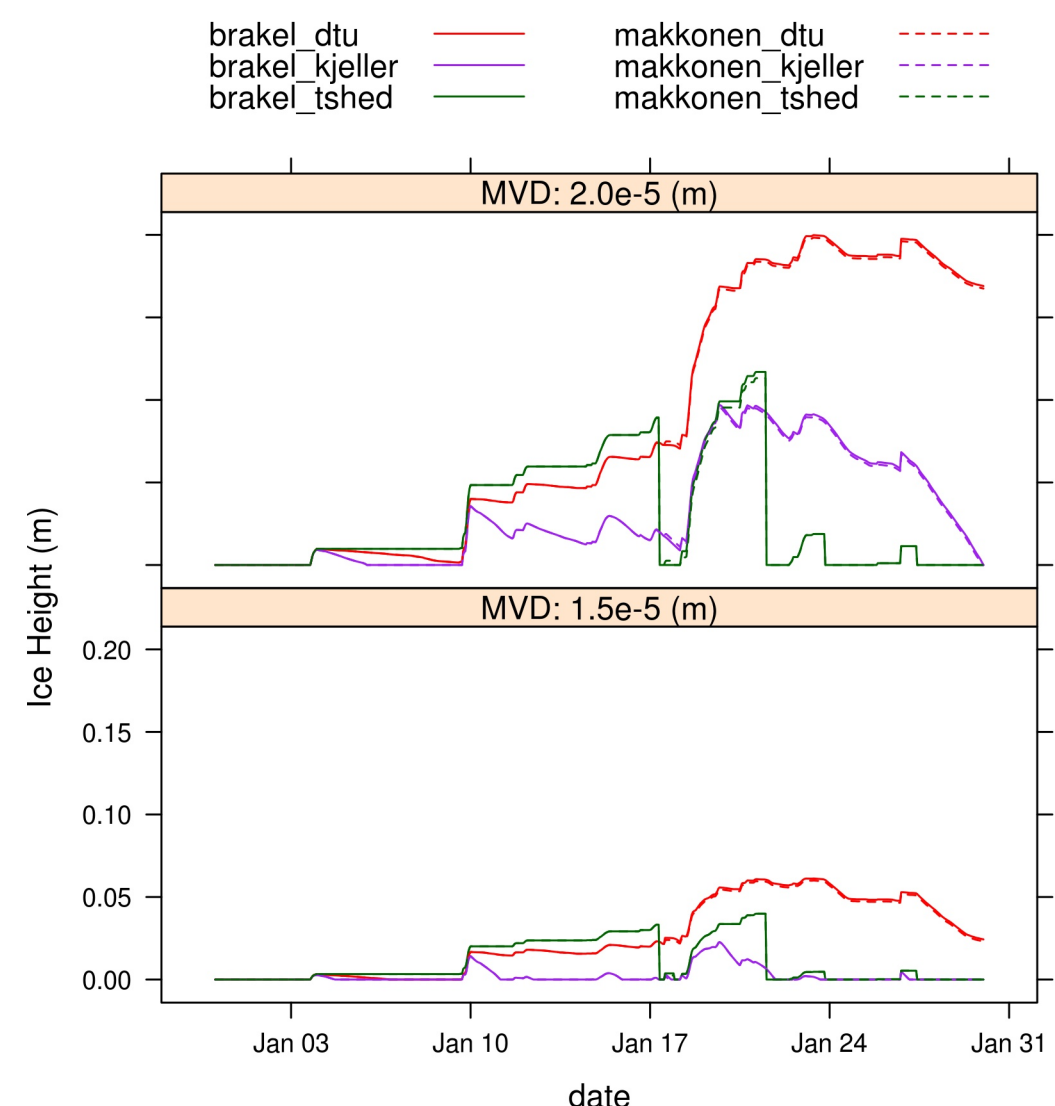


Figure 8. Timeseries of ice amount at the leading edge of a wind turbine blade using different icing models. All icing models forced using data from the Thompson / MYNN2 simulations.

Figure 8 shows a comparison of the 6 different icing models with time. It shows almost no difference between the two accretion models, however there is a large difference between the three ablation models.

During cold temperatures, the Kjeller method removes the most ice. When the temperature is above freezing, there is a dramatic loss of ice in the shedding model. During the first half of the month the models show ice during most of the same times, however the second half of the month shows very little ice in the tshed based models, while the other two ablation models still show large amounts of ice.

The two MVD sizes show an almost 4 times difference in the amount of ice which has accumulated when the droplet size is estimated to be 5 microns larger (upper plot) than in the lower plot.

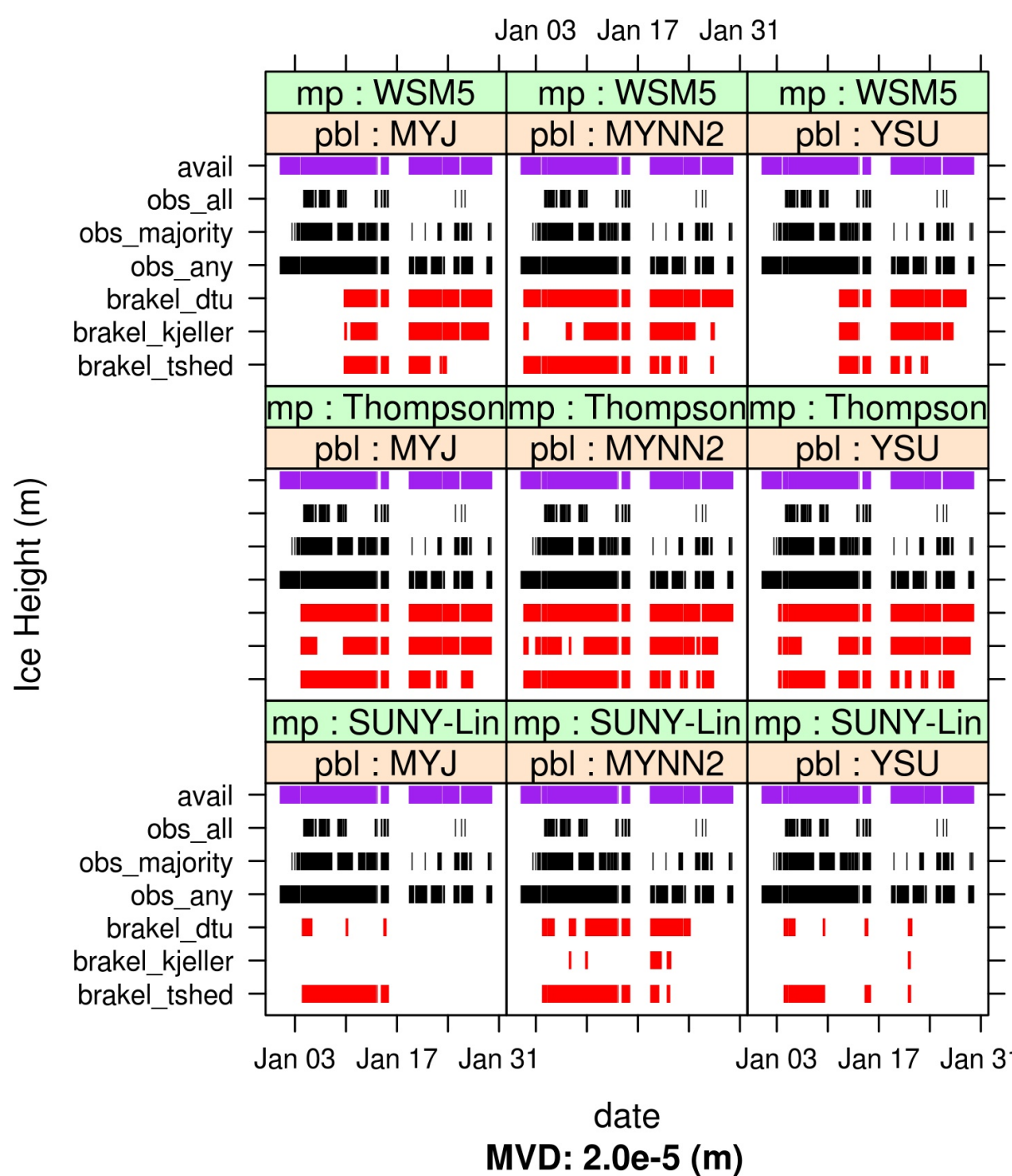


Figure 9. Timeseries of icing events, signified by any icing amount. Different boxes show the different WRF sensitivities.

Figure 9 shows the model evaluated against our best guess for observed icing on the turbine.

The choice of both the microphysics scheme and PBL scheme are key to icing model results. SUNY-Lin does the poorest job capturing the low level clouds needed to generate icing at wind turbine heights, while Thompson does the best. The MYNN2 PBL scheme shows the earliest onset of icing, while the YSU scheme being the warmest melts ice too quickly at times.

When evaluating the icing models, the tshed ablation model performs the best capturing the lac of ice on the majority of the turbines at the end of the period.

References

Brakel, T. W., J. P. F. Charpin, and T. G. Myers. 2007. One-dimensional ice growth due to incoming supercooled droplets impacting on a thin conducting substrate. International Journal of Heat and Mass Transfer, 50, 1694–1705. doi:10.1016/j.jheatmasstransfer.2006.10.014.
Cattin, R., S. Kunz, A. Heimo, G. Russi, M. Russi, and M. Tiefgraber. 2007. Wind turbine ice throw studies in the Swiss Alps. European Wind Energy Conference Milan, Vol. 1 of, 3–7.
Laakso, T. and Coauthors. 2010. State-of-the-art of wind energy in cold climates. VTT, Finland.
Makkonen, L. 2000. Models for the growth of rime, glaze, icicles and wet snow on structures. Philosophical Transactions of the Royal Society of London. Series A: Mathematical, Physical and Engineering Sciences, 358, 2913–2939.